NO-REFERENCE QUALITY ASSESSMENT OF CAMERA-CAPTURED IMAGES

Lijuan Tang [†§], Leida Li [†], Ke Gu [‡], Jiansheng Qian [†], and Jianying Zhang [†]

† School of Info. and Elec. Eng., China Univ. of Mining and Technology, China
‡ School of Computer Science and Engineering, Nanyang Technological Univ., Singapore
§ School of Info. and Elec. Eng., Jiangsu Vocational College of Business, China
Email: nttlj@163.com

ABSTRACT. In this paper we address the problem of quality assessment of camera images from three types of features. The first type of features measures the naturalness of an image, inspired by a recent finding that there exists high correlation between structural degradation information and free energy entropy on natural scene images and this regulation will be gradually devastated as more distortions are introduced. The second type of features comes from an observation that a broad spectrum of statistics of distorted images can be caught by the generalized Gaussian distribution (GDD) according to natural scene statistics (NSS). The two types of features are based on NSS regulations, but they come from the considerations of local auto-regression and global histogram, respectively. The third type of features estimates the local sharpness computing log-energies in the discrete wavelet transform domain. Finally our quality metric is achieved via an SVR-based machine learning tool and its performance is proved to be statistically better than state-of-the-art competitors on the CID2013 database which is dedicated to the quality assessment of camera images.

Keywords: Quality assessment, camera images, no-reference, natural scene statistics, local sharpness, free energy theory, structural degradation model

1 Introduction

With the soaring development of mobile devices and network, an enormous amount of images are being presented to users every moment. It is challenging to evaluate and control the quality of digital photographs. At the same time, a supreme effort is still made by camera manufacturers to improve the quality of photography. As thus, it is in an urgent pursuit of finding ways to automatically predict the perceptual quality of camera images.

In the past few years, as for the issue of image quality assessment (IQA), many objective metrics of the ability to faithfully evaluate the quality of distorted images have been developed. If the distortion-free image which distorted image can be compared with is available, the metric is called full-reference (FR) IQA [1]. But in most

Lijuan Tang and Prof. Jianying Zhang have the same contribution to this paper.

cases only the distorted image is available, this type of IQA models are called no-reference (NR) IQA. Furthermore, according to the requirement of prior knowledge of the images or their distortions, current NR-IQA algorithms also can be further classified into two categories, namely general-purpose metrics and distortion-specific metrics. Typical distortion-specific blind quality measures are devoted to blockiness [2], noise [3], tone mapping [4], retargeting [5], enhancement [6-8], sharpness/blurriness [9-15], etc. In recent years, general-purpose NR-IQA metrics have been an active research field [16-24].

Although aforementioned metrics perform well on the popular databases such as the LIVE database [25], they do not perform as well on real photographs which are subjected to many different distortion sources and types. Because these image quality metrics have been based on the assumption that an image contains single or simulated distortions which are not representative of what one encounters in practical real scenarios [26]. Camera images contain more practical distortions unlike most distortions present in the popular databases. Compared with the previous works, to the best of our knowledge, this paper is the first to propose to a modular framework for IQA of camera images based on the NSS regulation and local sharpness assessment. And furthermore, the proposed blind quality index for camera images (BQIC) has acquired substantially high performance, it is the only metric with the correlation coefficient of beyond 80% in both linear and monotonic performance indices.

The paper is structured below. In section II, we present the details of the BQIC algorithm. Section III compares performance measures of our BQIC and state-of-the-art blind quality metrics on the CID2013 database [27] that is dedicated to the IQA of camera images. Conclusion and future works are provided in Section IV.

2 No-Reference quality metric of camera-captured images

Selecting appropriate features plays an important part in IQA problems. The features of the proposed metric consist of three parts. The flowchart of the proposed NR-IQA metric is shown in Fig. 1.

The first group of features is extracted based on the free-energy principle, which is recently found in brain theory and neuroscience [21], and structural degradation measurement via simple convolutions and nonlinear regression [28]. The free-energy principle operates under the assumption that there always exists a difference between an input genuine visual signal and its processed one by human brain. Human perceptual process is manipulated by an internal generative model, which can infer predictions of the input visual signal and avoid the residual uncertainty information. On this basis, the psychovisual quality of a scene is defined by both the scene itself and the output of the internal generative model. It differs from most traditional methods which are based on signal decomposition. In this paper we choose the linear AR model as the generative model for its effectiveness and simplicity to describe natural scenes [15, 22, 24]. The AR model is defined as

$$y_n = \varphi^k(y_n)\theta + \epsilon_n \tag{1}$$

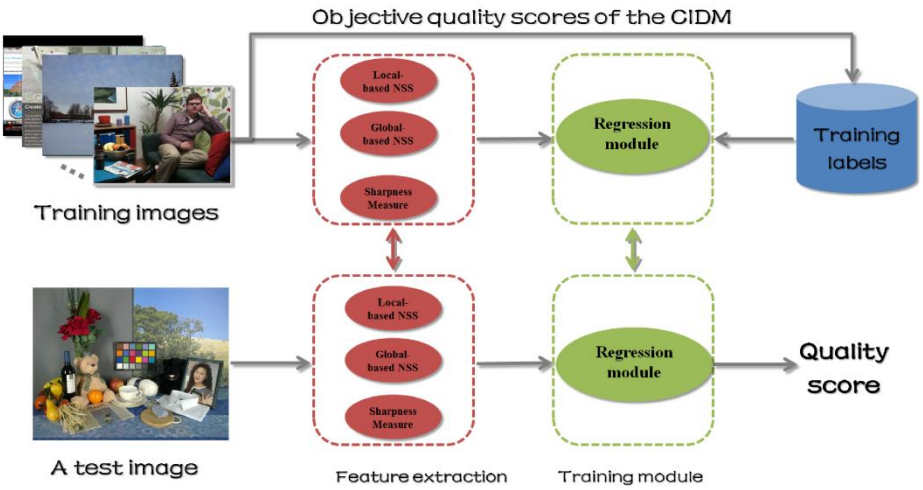

Fig. 1. The framework of the proposed NR-IQA metric.

where y_n is a pixel of the distorted image, $\varphi^k(y_n)$ is a row-vector consisting of k nearest neighbors of y_n , $\theta = (\theta_1, \theta_2, \ldots, \theta_k)^T$ is a vector of AR coefficients, and ϵ_n is the error term. Then, the predicted version of the input distorted visual signal I can be estimated by $\varphi^k(y_n)\ \theta_{opt}$, where θ_{opt} is the optimal estimate of AR parameters for y_n based on the least square method.

It is known that low-pass filtered versions of the distorted images have different degrees of spatial frequency decrease. The reduced-reference structural degradation model (SDM) [28] measures the similarity information between original and distorted images. We modify the classical SSIM [30], and define the structural degradation information to be:

$$S(I) = E\left(\frac{\sigma_{(\mu_I \overline{\mu_I})} + C}{\sigma_{(\overline{\mu_I})}\sigma_{(\mu_I)} + C}\right) \tag{2}$$

where μ_I represents the mean intensity, $\sigma_{(\mu_I \overline{\mu_I})}$ indicates the local covariance the same as the definition in SSIM [30]; E(•) is a direct average pooling; C is a small constant to avoid instability when denominator is very close to zero. Because different sizes of Gaussian weighting functions introduce different amounts information, this paper picks three pairs of (*K*, *L*) as (1, 1), (3, 3) and (5, 5). And for noise images of poorer quality, SDM's predictions are quite distinct for subjective scores. We thereby modify *S*(*I*) to keep different types of distortions consistent:

$$\tilde{S}(I) = \begin{cases} -S(I) & if\ F(I) > T \\ S(I) & otherwise \end{cases} \tag{3}$$

where the threshold T = 5 is chosen empirically to avoid SDM's predicted scores being not consistent with the quality of image for specific distortion types, e.g. noise and blur. We redefine $\tilde{S}$ for different values of (*K*, *L*) with *K* = *L* =1, *K* = *L* = 3 and *K*

= L = 5. An approximate linear relationship between the structural degradation information and the free energy feature of original image can be found on thirty images which are randomly selected from Berkeley database [31] and draw the scatter plots in Fig. 2. The linear dependence feature provides possibility to describe distorted images without primitive image. We define the linear regression model as follows:

$$F(I_r) = \alpha \cdot \tilde{S}(I_r) + \beta \tag{4}$$

Where I_r indicates the original image, α and β are gained by the least square algorithm. We then reduce the dependence of original references by using $FS_I = F(I_d) - \{\alpha \cdot \tilde{S}(I_d) + \beta)\}$ to be defined as the features, where I_d indicates the distorted image. Note that FS_I values of high-quality images are quite near to zero, and conversely they will be far from zero when distortions are progressively intensive. Finally, we supplement the free energy entropy as the final feature of group one, because it delivers good performance on noisy and blurred images.

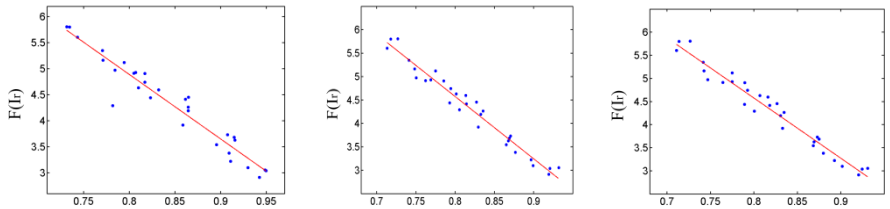

$\widetilde{S_1}(I_r)$ $\widetilde{S_3}(I_r)$ $\widetilde{S_5}(I_r)$

Fig. 2. Scatter plots of the structural degradation information $\widetilde{S_s}(I_r)$ (s = {1, 3, 5}) vs. the free energy feature F(I_r) on thirty images in the Berkeley database [31]. The straight lines are fitted with the least square method.

The second type of features comes from a classical NSS based model [28, 30]. We can estimate decorrelating effect by exerting a local non-linear operation on log-contrast luminance to remove local mean displacements from zero log-contrast and to normalize the local variance of the log-contrast, as used in some popular blind IQA techniques [16-18, 22]. It was found that the normalized luminance value of natural images without distortions appears Gaussian characteristic [32], and the distribution is broken when the images suffer distortions. However, a wider spectrum of statistics of distorted images can be effectively caught by the generalized Gaussian distribution (GGD). The probability density function of GGD defined as following:

$$f(x;\mu,\alpha,\beta) = \frac{\alpha}{2\beta\gamma(\frac{1}{\alpha})} exp\left(-\left(\frac{|x-\mu|}{\beta}\right)^{\alpha}\right) \quad \alpha > 0 \tag{5}$$

where μ is the mean, α is the shape parameter that controls the 'shape' of the distribution

$$\beta = \sigma \sqrt{\frac{\gamma(\frac{1}{\alpha})}{\gamma(\frac{3}{\alpha})}} \tag{6}$$

and the gamma function $\gamma(\cdot)$ is given by:

$$\gamma(z) = \int_0^\infty t^{z-1} e^{-t} dt \tag{7}$$

where the parameter σ is defined to be standard deviation. In this paper, we deploy the GGD with zero mean to fit the mean subtracted contrast normalized (MSCN), because MSCN is global-based NSS and MSCN coefficient distributions are symmetric [32]. The GGD with zero mean is defined as following:

$$f(x; \alpha, \beta) = \frac{\alpha}{2\beta\gamma(\frac{1}{\alpha})} exp\left(-\left(\frac{|x|}{\beta}\right)^\alpha\right) \tag{8}$$

For every image, two pairs of parameters (α, σ^2) from a GGD fit of the MSCN coefficients. One pair is from the original scale, another is at the reduced resolution via a low-pass filtering by a down sampling with the factor of 2. These form the second group of four features which will be used to capture image distortion.

The third group of features is the modified patch-based image sharpness measure [10]. First, using Cohen-Daubechies-Feauveau filters [33] to decompose the input image signal into discrete wavelet transform (DWT) subbands only with one level. Then computing the Log-energy of each subband of discrete wavelet transform (DWT) as follows:

$$E_{xy} = log_{10}(1 + \frac{1}{M}\sum_{i,j} S_{XY}^2(i,j)) \tag{9}$$

where S_{XY} is either S_{HH}, S_{HL} or S_{LH}, and S_{LL} is not used, and M is the number of DWT coefficients in the subband. The addition of one is used to avoid negative values of E_{XY}. In [10], the authors measured the total log-energy at each level via

$$E_n = (1-\alpha)\frac{E_{LHn}+E_{HLn}}{2} + \alpha E_{HHn} \tag{10}$$

where the parameter α is 0.8. But according to [34], the authors used predictable sinusoidal, triangular target motions and randomized step-ramp stimuli to compare smooth pursuit in the horizontal and vertical planes. It is confirmed that most normal subjects show higher gain values during horizontal than during vertical tracking. Grönqvist [35] also observed that vertical tracking inferior to horizontal tracking and the proportion of smooth pursuit increased with age. So horizontal tracking and vertical tracking are asymmetry. Thorough experiments are performed to give the result that LH, HL and HH appears auto-adaptive non-linear relationship. Hence we separately consider using E_{LHn}, E_{HLn} and E_{HHn} as features, instead of directly combining them via Eq. (10). Finally, we use the above algorithm in a block-based way to obtain the sharpness index across the entire image. The block-based procedure is similar to that in [10]. A collection of local sharpness values are computed using the DWT coefficients associated to each 16×16 block of the image, and the index is computed by taking the root mean square of the 1% largest values of the block sharpness indices.

After feature extraction, we need to find a proper way that can map the feature space to subjective MOS, then utilize it to produce objective quality scores. In order to make a fair comparison with other NR-IQA methods, we use a support vector regression module SVR [37] to generate a proper mapping that is learnt from the feature score to human visual system. SVR has been widely used in the IQA field [22]. Here the SVR with a radial basis function (RBF) is adopted by using the LIBSVM package [37].

3 Experimental results

In this section, the CID2013 database [27] is used as testing bed for performance evaluation and comparison. The CID2013 database includes 6 image sets with 36 scenarios and associated 474 distorted images captured by 79 distinct digital cameras. The images in the CID2013 database don't have reference images because they were captured by real cameras, which make FR- and RR-IQA methods barely work. As for our training-based BQIC algorithm, we use a similar method to what is used in [38]. To be specific, the predicted rating for each image was determined by training an SVR on 473 images via a leave-one-out cross-validation methodology [38]. We will test the performance of the proposed blind BQIC metric from two aspects. The first is to demonstrate the effectiveness of our BQIC method compared to state-of-the-art general-purpose NR-IQA metrics. And the second is to analyze and compare the effectiveness of our BQIC method compared to state-of-the-art specific-distortion NR-IQA metrics. In this paper we follow the video quality experts group (VQEG)'s suggestion and employ a five-parameter nonlinear fitting function to map objective quality scores to subjective human ratings [39]. Then, four performance measures, including SRCC, KRCC, PLCC and RMSE, are exploited.

Recently, popular general-purpose NR-IQA metrics have been proposed to evaluate distorted images without knowing the distortion types. Later we will demonstrate and compare the performance of the proposed model with the top general-purpose NR-IQA approaches, BLIINDS-II [17], BRISQUE [18], SISBLIM [19], NFERM [22], and IL-NIQE [29]. A logistic nonlinear function is used before calculating PLCC and RMSE. Table I summarizes the performance results on the CID2013 database. One can see from Table I that the proposed BQIC metric has achieved the highest PLCC, SRCC and KRCC values as well as the smallest RMSE value. None of the compared metrics performs better than the proposed metric, namely the proposed BQIC model correlates highly with human visual perception to image distortions. We also show the scatter plots of the subjective scores versus the predicted scores using different metrics in Fig. 3. A good metric is expected to produce scatter points that are closed to the fitted curve. It can be easily found from Fig. 3 that the proposed metric produces the best fitting results on the CID2013 database.

Sharpness is one of the most important factor in the problem of quality assessment of camera images. In this section, we will demonstrate and compare the performance of the proposed model with 5 popular blind sharpness algorithms BLUR [9], S_3 [14], FISH [10], $FISH_{bb}$ [10], and ARISM [15]. To estimate the performance of the

Table 1. Comparison of our BQIC metric and state-of-the-art general-purpose NR-IQA methods on CID2013. We bold the best performed NR IQA algorithm.

CID2013	PLCC	SRCC	KRCC	RMSE
BLIINDS-II	0.6385	0.6346	0.4539	17.4254
BRISQUE	0.7810	0.7844	0.5902	14.1405
SISBLIM	0.7008	0.6534	0.4763	16.0973
NFERM	0.7933	0.7880	0.5943	13.7836
IL-NIQE	0.4268	0.3065	0.2101	20.4744
BQIC	**0.8283**	**0.8207**	**0.6291**	**12.6852**

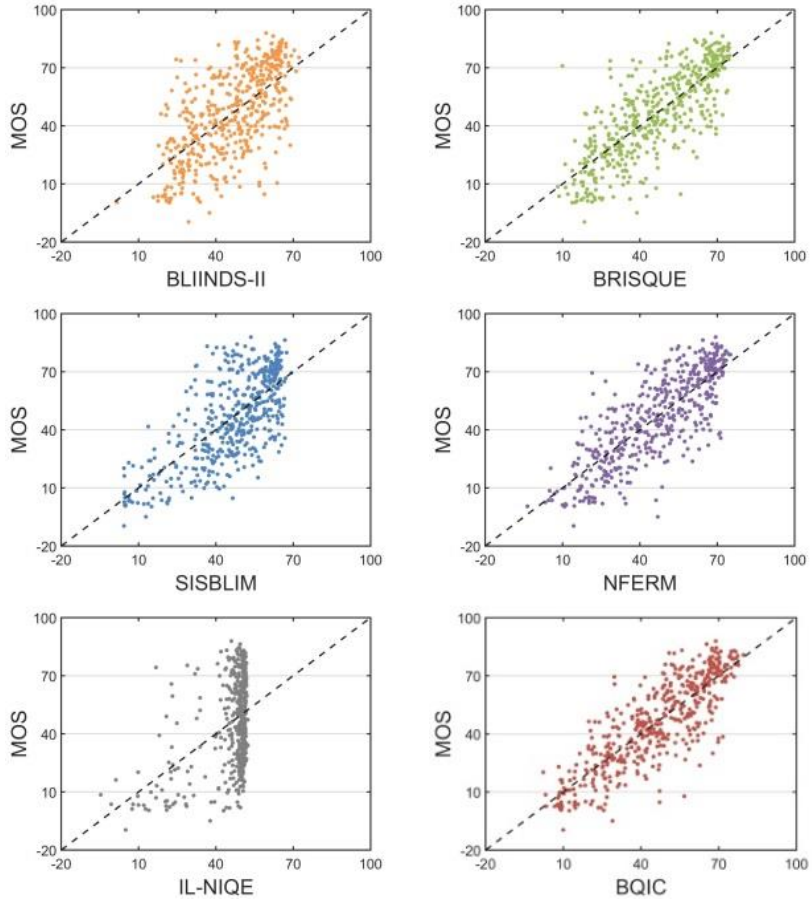

Fig. 3. Scatter plots of objective scores generated by BLIINDS-II, BRISQUE, SISBLIM, NFERM, IL-NIQE and our proposed BQIC metric versus subjective scores reported by CID2013 databases after nonlinear mapping.

Table 2. Comparison of our BQIC metric and state-of-the-art distortion-specific blind algorithms on CID2013. We bold the best performed NR IQA model.

CID2013	PLCC	SRCC	KRCC	RMSE
BLUR	0.5182	0.5515	0.4063	19.3009
S_3	0.3270	0.2936	0.2019	21.3958
FISH	0.6858	0.6749	0.4925	16.4764
$FISH_{bb}$	0.7549	0.7383	0.5461	14.8480
ARISM	0.4877	0.4408	0.3090	19.7651
BQIC	**0.8283**	**0.8207**	**0.6291**	**12.6852**

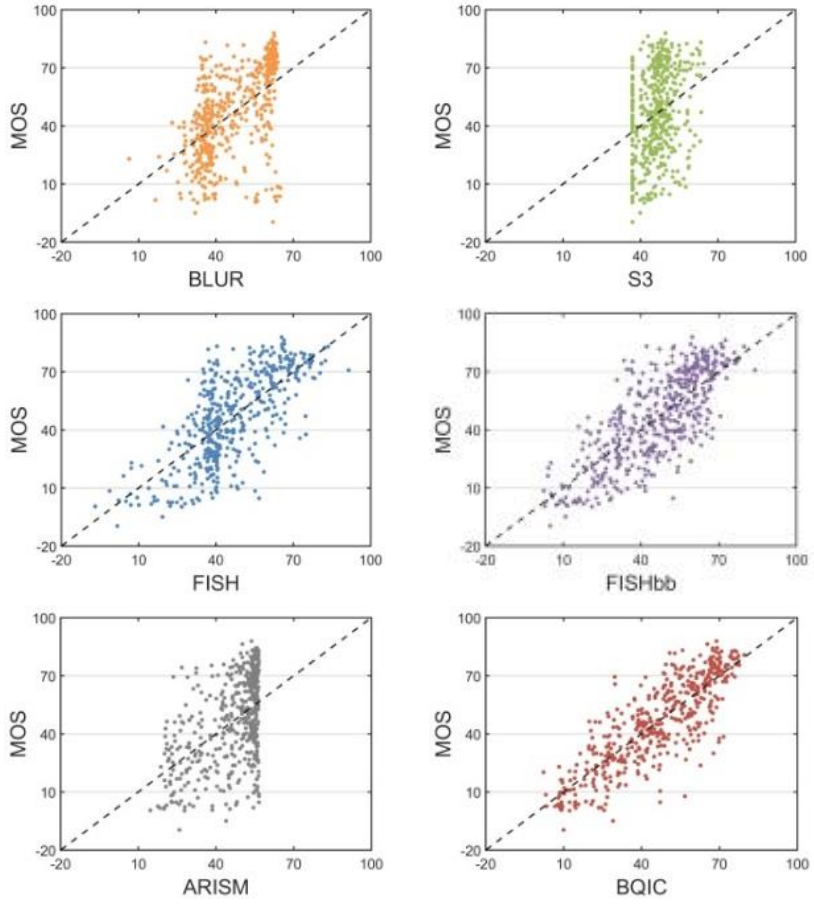

Fig. 4. Scatter plots of objective scores generated by BLUR, S_3, FISH and $FISH_{bb}$, ARISM and our proposed metric BQIC versus subjective scores reported by CID2013 databases after non-linear mapping.

proposed BQIC metric and aforementioned specific-distortion blind algorithms, experiments are conducted on the CID2013 database. Table II lists the performance of the comparison methods and Fig. 4 shows the scatter plots between the predicted scores and the corresponding MOSs on the CID2013 database, where a point denotes one image. It can be found that the proposed algorithm not only competes with these specific-distortion metrics, but also outperforms it.

4 Conclusion

With the development of networked hand-held devices, a large amount of visual data is presented to users. Many efforts have been made to ensure the end consumers are presented with a satisfactory quality of experience (QoE). Therefore, assessment of camera images is a significant and meaningful topic in scientific research and applicational development of digital image processing. However, it is struggle to handle the images with many concurrent distortion types for current blind quality metrics. Effective objective quality metrics are expected.

In this paper we have put forward a blind quality index for camera images with natural scene statistics and patch-based sharpness assessment. A comparison of our BQIC with state-of-the-art general-purpose NR-IQA methods and popular blind distortion-specific measures is conducted on CID2013 database. The experiment results have proved the superior performance of the proposed blind quality measure on the CID2013 database. Besides the substantially high prediction accuracy, it is worthy to emphasize three points below. First, experimental results prove the superiority of our proposed method on CID2013 over popular NR-IQA models and blind sharpness measures. Second, the proposed BQIC needs merely 11 features, far less than the majority of general-purpose train-based NR-IQA metrics. Third, to the best of our known, our proposed method is the first to propose modular framework for camera images based on nature scene statistics and sharpness assessment.

5 REFERENCES

1. W. Lin, C.-C. Jay Kuo, “Perceptual visual quality metrics: A survey,” J. Vis. Commun. Image Represent., vol. 22, no. 4, pp. 297-312, May. 2011.
2. S. A. Golestaneh, D. M. Chandler, “No-reference quality assessment of JPEG images via a quality relevance map,” IEEE Sig. Process. Lett., vol. 21, no. 2, pp. 155-158, Feb. 2014.
3. D. Zoran, Y. Weiss, “Scale invariance and noise in natural images,” in Proc. IEEE Int. Conf. Comput. Vis., pp. 2209-2216, Sept. 2009.
4. K. Gu, S. Wang, G. Zhai, S. Ma, X. Yang, W. Lin, W. Zhang, W. Gao, “Blind quality assessment of tone-mapped images via analysis of information, naturalness and structure,” IEEE Trans. Multimedia, vol. 18, no. 3, pp. 432-443, Mar. 2016.
5. Y. Fang, K. Zeng, Z. Wang, W. Lin, Z. Fang, C.-W. Lin, “Objective quality assessment for image retargeting based on structural similarity,” IEEE J. Emerg. Sel. T. Circuits Syst., vol. 4, no. 1, pp. 95-105, Mar. 2014.

6. S. Wang, K. Gu, S. Ma, W. Lin, X. Liu, W. Gao, “Guided image contrast enhancement based on retrieved images in cloud,” IEEE Trans. Multimedia, vol. 18, no. 2, pp. 219-232, Feb. 2016.
7. K. Gu, G. Zhai, X. Yang, W. Zhang, C. W. Chen, “Automatic contrast enhancement technology with saliency preservation,” IEEE Trans. Circuits Syst. Video Technol., vol. 25, no. 9, pp. 1480-1494, Sept. 2015.
8. K. Gu, G. Zhai, W. Lin, M. Liu, “The analysis of image contrast: From quality assessment to automatic enhancement,” IEEE Trans. Cybernetics, vol. 46, no. 1, pp. 284-297, Jan. 2016.
9. P. Marziliano, F. Dufaux, S. Winkler, T. Ebrahimi, “Perceptual blur and ringing metrics: Application to JPEG2000,” Sig. Process. Image Commun., vol. 19, no. 2, pp. 163-172, Feb. 2004.
10. P. V. Vu, D. M. Chandler, “A fast wavelet-based algorithm for global and local image sharpness estimation,” IEEE Sig. Process. Lett., vol. 19, no. 7, pp. 423-426, Jul. 2012.
11. L. Li, W. Lin, X. Wang, G. Yang, K. Bahrami, A. C. Kot, “No reference image blur assessment based on discrete orthogonal moments,” IEEE Trans. Cybernetics, vol. 46, no. 1, pp. 39-50, Jan. 2016.
12. R. Ferzli, L. J. Karam, “A no-reference objective image sharpness metric based on the notion of just noticeable blur (JNB),” IEEE Trans. Image Process., vol. 18, no. 4, pp. 717-728, Apr. 2009.
13. N. D. Narvekar, L. J. Karam, “A no-reference image blur metric based on the cumulative probability of blur detection (CPBD),” IEEE Trans. Image Process., vol. 20, no. 9, pp. 2678-2683, Sept. 2011.
14. C. T. Vu, T. D. Phan, D. M. Chandler, “S3: A spectral and spatial measure of local perceived sharpness in natural images,” IEEE Trans. Image Process., vol. 21, no. 3, pp. 934-945, May. 2012.
15. K. Gu, G. Zhai, W. Lin, X. Yang, W. Zhang, “No-reference image sharpness assessment in autoregressive parameter space,” IEEE Trans. Image Process., vol. 24, no. 10, pp. 3218-3231, Oct. 2015.
16. A. Mittal, R. Soundararajan, A. C. Bovik, “Making a completely blind Image quality analyzer,” IEEE Sig. Process. Lett., vol. 20, no. 3, pp. 209-212, Mar. 2013.
17. M. A. Saad, A. C. Bovik, “Blind image quality assessment: A natural scene statistics approach in the DCT domain,” IEEE Trans. Image Process., vol. 21, no. 8, pp. 3339-3352, Aug. 2012.
18. A. Mittal, A. K. Moorthy, A. C. Bovik, “No-reference image quality assessment in the spatial domain,” IEEE Trans. Image Process., vol. 21, no. 12, pp. 4695-4708, Dec. 2012.
19. K. Gu, G. Zhai, X. Yang, W. Zhang, “Hybrid no-reference quality metric for singly and multiply distorted images,” IEEE Trans. Broadcasting, vol. 60, no. 3, pp. 555-567, Sept. 2014.
20. A. K. Moorthy, A. C. Bovik, “Blind image quality assessment: From natural scene statistics to perceptual quality,” IEEE Trans. Image Process., vol. 20, no. 12, pp. 3350-3364, Dec. 2011.
21. G. Zhai, X. Wu, X. Yang, W. Lin, W. Zhang, “A psychovisual quality metric in free-energy principle,” IEEE Trans. Image Process., vol. 21, no.1, pp. 41-52, Jan. 2012.
22. K. Gu, G. Zhai, X. Yang, W. Zhang, “Using free energy principle for blind image quality assessment,” IEEE Trans. Multimedia, vol. 17, no. 1, pp. 50-63, Jan. 2015.
23. Y. Fang, K. Ma, Z. Wang, W. Lin, Z. Fang, G. Zhai, “No-reference quality assessment of contrast-distorted images based on natural scene statistics,” IEEE Sig. Process. Lett., vol. 22, no. 7, pp. 838-842, Jul. 2015.

24. K. Gu, G. Zhai, W. Lin, X. Yang, W. Zhang, “Learning a blind quality evaluation engine of screen content images,” Neurocomputing, vol. 196, pp. 140-149, Jul. 2016.
25. H. R. Sheikh, Z. Wang, L. Cormack, A. C. Bovik, “LIVE image quality assessment Database Release 2,” [Online]. Available: http://live.ece.utexas.edu/research/quality.
26. M. A. Saad, P. Corriveau, R. Jaladi. “Objective consumer device photo quality evaluation,” IEEE Sig. Process. Lett., vol. 22, no. 10, pp. 1516-1520, Oct. 2015.
27. T. Virtanen, M. Nuutinen, M. Vaahteranoksa, P. Oittinen, J. Hakkinen, “CID2013: A database for evaluating no-reference image quality assessment algorithms,” IEEE Trans. Image Process., vol. 24, no. 1, Jan. 2015.
28. K. Gu, G. Zhai, X. Yang, W. Zhang, “A new reduced-reference image quality assessment using structural degradation model,” in Proc. IEEE Int. Symp. Circuits and Syst., pp. 1095-1098, May. 2013.
29. L. Zhang, L. Zhang, A. C. Bovik, “A feature-enriched completely blind image quality evaluator,” IEEE Trans. Image Process., vol. 24, no. 8, pp. 2579-2591, Aug. 2015.
30. Z. Wang, A. C. Bovik, H. R. Sheikh, E. P. Simoncelli, “Image quality assessment: From error visibility to structural similarity,” IEEE Trans. Image Process., vol. 13, no. 4, pp. 600-612, Apr. 2004.
31. D. Martin, C. Fowlkes, D. Tal, J. Malik, “A database of human segmented natural images and its application to evaluating segmentation algorithms and measuring ecological statistics,” in Proc. IEEE Int. Conf. Comput. Vis., pp. 416-423, 2001.
32. D. L. Ruderman, “The statistics of natural images,” Netw. Comput. Neural Syst., vol. 5, no. 4, pp. 517-548, 1994.
33. A. Cohen, I. Daubechies, J.-C. Feauveau, “Biorthogonal bases of compactly supported wavelets,” Commun. Pure Appl. Math., vol. 45, Jun. 1992.
34. K. G. Rottach et al., “Comparison of horizontal, vertical and diagonal smooth pursuit eye movements in normal human subjects,” Vision Research, vol. 36, no. 14, pp. 2189-2195, Jul. 1996.
35. H. Grönqvist, G. Gredeback, C. V. Hofsten, “Developmental asymmetries between horizontal and vertical tracking,” Vision Research, vol.46, no.11, pp.1754-1761, May 2006.
36. B. Schokopf, A. J. Smola, R. C. Williamson, P. L. Bartlett, “New support vector algorithms,” Neural Comput. , vol. 12, no. 5, pp. 1207-1245, 2000.
37. C-C. Chang, C-J. Lin, “LIBSVM: a library for support vector machines,” ACM Trans. Intelligent Symp. Technol., vol. 2, no. 3, 2011.
38. E. Kee, H. Farid, “A perceptual metric for photo retouching,” Proceedings of the National Academy of Sciences of the United States of America., vol. 108, no. 50, pp. 19907-19912, Dec. 2011.
39. VQEG, “Final report from the video quality experts group on the validation of objective models of video quality assessment,” Mar. 2000, http://www.vqeg.org/.